J Appl Electrochem (2011) 41:657–662
DOI 10.1007/s10800-011-0284-1

ORIGINAL PAPER

Deposition of titanium on SiC fibres from chloride melts

Joachim G. Gussone · Joachim M. Hausmann

Received: 23 November 2010 / Accepted: 24 February 2011 / Published online: 18 March 2011

Abstract The present study examined the feasibility of producing titanium matrix composites based on a molten salt fibre coating process. It is demonstrated that sufficiently thick and coherent titanium coatings can be deposited on SiC fibres in LiCl–KCl–$TiCl_2$ at 700 K. One important aspect of the study was the behaviour of the substrate during electrolysis. Therefore, additional features related to carbon-coated SiC fibres and carbonaceous substrates in general are outlined. The morphologies and microstructures of electrolytically coated SiC fibres were investigated by scanning electron microscopy and compared to fibres coated by a physical vapour deposition technique. The cause and relevance of the growth failures that were observed in this study are also discussed.

Keywords Titanium matrix composites · Silicon carbide fibre · Carbonaceous substrates · Lithium intercalation · Titanium carbide · Growth failures

1 Introduction

Titanium matrix composites (TMCs) are high-performance materials that are intended for aerospace applications. Depending on the titanium alloy used as the matrix material, TMCs can offer high specific strength and stiffness at temperatures up to 600 °C [1]. Over the last two decades, various production routes have been studied by several institutions [2]. The most prominent methods are the foil–fibre–foil (FFF) process and monotape techniques (e.g. the plasma spray process). High-quality TMCs with excellent fibre distribution and interface properties have been produced according to the matrix coated fibre (MCF) concept using physical vapour deposition (PVD) with magnetron sputter technology [1]. In these studies [1], the MCFs were stacked, encapsulated and pressed for consolidation by hot isostatic pressing (HIP) so that the coating formed a continuous matrix material. However, the production costs were very high, especially for the fibre coating. Therefore, cost-efficient processes based on the electrodeposition of titanium in molten salts are presently studied. This type of electrolytical production route has not been proposed yet, but Lantelme et al. [3] studied the electrodeposition of niobium on SiC filaments from NaCl–KCl–NaF–K_2NbF_7 to produce TMCs via the FFF technique. Niobium was intended to diffuse into the titanium matrix and work as a crack arrester. The fundamental aspects of the electrochemistry and electrodeposition of titanium in molten salts have been investigated by several authors [4–9] and are not reproduced here. For more information, a review by Girginov et al. [10] should be consulted.

The aim of this paper was to examine the influence of the substrate SCS-6 on the deposition process. The structure and mechanical properties of SCS-6, a composite material from Specialty Materials Inc., consisting of β-SiC grown on 30-μm thick pitch-based carbon filaments, have been extensively investigated [11, 12]. The electrical properties are governed by the outer carbonaceous coating, which means that no specific resistivity can be specified. Specialty Materials Inc., however, determined the

J. G. Gussone (✉) · J. M. Hausmann
German Aerospace Center (DLR), Institute of Materials Research, Linder Höhe, 51147 Cologne, Germany
e-mail: joachim.gussone@dlr.de

dependence between length and resistance and calculated a quasi-specific resistivity (approximately 0.012 Ω cm).[1] As this resistivity impeded proper electrochemical measurements, glassy carbon (GC), which has a higher specific conductivity[2] and can be applied with larger diameters, was also studied as a reference for SCS-6. An "ideal" substrate would neither react with the electrolyte nor form an alloy with titanium during electrodeposition. Tungsten is one element that meets these requirements, so tungsten wires were used for comparison.

2 Experimental

All experiments were carried out in a glovebox system (Jacomex) with a controlled atmosphere of high-purity argon (H_2O, $O_2 < 1$ ppm). Chemicals, electrodes and crucibles were handled and stored within the glovebox to minimise humidity in the cell. The molten salt reactor, which was attached to the working chamber of the glovebox via a gas-tight connection, was also used to dry the salts under vacuum or high-purity argon. An eutectic mixture of separately dried KCl (Fluka puriss. p.a., ACS reagent, >99.0%) and LiCl (Fluka puriss. p.a., ACS reagent, >99.0%, anhydrous) served as the base electrolyte at temperatures between 650 and 800 K. Titanium(II) chloride (Sigma-Aldrich, 99.98%, anhydrous) was used without further treatment at concentrations between 0.1 and 1 mol%. Working electrodes (WE) made of tungsten wires (approximately 0.14 mm), SCS-6 fibres and GC rods (Sigradur® G, 4 mm) were fixed onto 1 mm tungsten wires above the fused salt level. Platinum, titanium or tungsten wires served as quasi-reference electrodes (QRE) and retained a sufficiently constant potential during the experiments. Electrochemical measurements, specifically cyclic voltammetry (CV) and electrodeposition experiments with constant or pulsed currents were performed using a BANK HC 400 potentiostat/galvanostat. The CV generally consisted of three cycles. In some cases, the reverse potentials were changed within one experiment. Morphology and microstructure of the deposits were analysed using optical microscopy and a Zeiss Ultra 55 scanning electron microscope (SEM) equipped with instrumentation (Oxford Instruments) for energy dispersive X-ray spectroscopy (EDS) and electron backscatter diffraction (EBSD).

[1] The conductivity of a copper wire with the same diameter (142 μm) and length would be almost four orders of magnitude higher.

[2] According to Dübgen and Popp [13], the specific resistivity of GC (Sigradur® G) is approximately 0.004 Ω cm.

3 Results

3.1 Electrochemical measurements

The first step in the course of the electrochemical measurements was to determine the influence of the substrate on the electrochemical window in $(LiCl–KCl)_{eut}$. Measurements with tungsten and boron-doped diamond (BDD) showed similar electrochemical windows (>3.6 V), and lithium deposition and chlorine evolution were observed.[3] Figure 1 shows that the electrochemical window was approximately 2 V and limited by lithium intercalation (R_2) when SCS-6 was used, which is even smaller than the electrochemical window for GC.

Reactions of titanium species were studied after the addition of $TiCl_2$. When tungsten was used, we observed the reactions that are characteristic of all-chloride melts with small cations (Fig. 2; Eq. 1).

$$\mathrm{Ti(IV)} \leftrightarrow \mathrm{Ti(III)} \leftrightarrow \mathrm{Ti(II)} \leftrightarrow \mathrm{Ti(s)} \quad (1)$$

Titanium deposition on tungsten started at approximately −2.2 V versus Cl_2/Cl^-, which was distinctively more negative than the value associated with the beginning of the lithium intercalation in the carbon coating of SCS-6. Thus, we suspected that intercalation processes can be coincident with Ti deposition on SCS-6.

At lower temperatures (≪800 K), the oxidation of trivalent titanium ions (peak O_2) resulted in unsolved products, which has also been reported in previous studies [7, 14, 15].[4] A transition observed in the current–voltage curve supported the findings of Ferry and Picard [16], who proved by impedance spectroscopy that tetravalent titanium dissolves as $(TiCl_6)^{2-}$ at lower current densities, whereas at higher current densities a solid layer of K_2TiCl_6 forms at the electrode. This reaction has no impact on the electrodeposition process and can be neglected for the consideration of suitable process parameters. However, at temperatures as low as 650 K and a concentration of 1 mol% $TiCl_2$, the appearance of the CV changed drastically, which indicated that precipitations had formed during reduction reactions at potentials close to the electrodeposition process. This observation was critical and marked a limit for the parameter range. Conversely, high temperatures are less favourable because of the increased reactivity of the melt and disproportionation reactions.

[3] Features related to passivation or anodic dissolution of tungsten (according to Lantalme and Salmi [5], at about −0.5 V versus Cl_2/Cl^-) and lithium intercalation in BDD at very negative potentials have also been observed in some cases, but will not be discussed here.

[4] The authors provided different explanations, such as the formation of solid Li_2TiO_3 or gaseous $TiCl_4$.

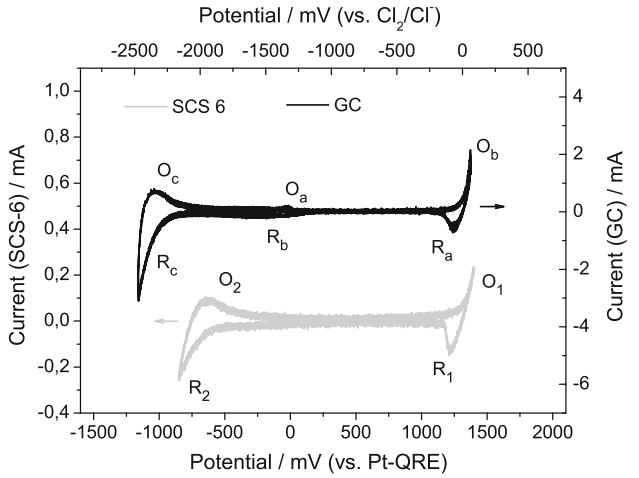

Fig. 1 CV in $(LiCl–KCl)_{eut.}$ at 700 K: comparison of the electrochemical windows (SCS-6, lower CV and GC, upper CV). The electrochemical windows are limited by chlorine evolution (O_b, O_1) and lithium intercalation (R_c, R_2). Further reactions (O_a, R_b) were probably caused by small amounts of oxide impurities

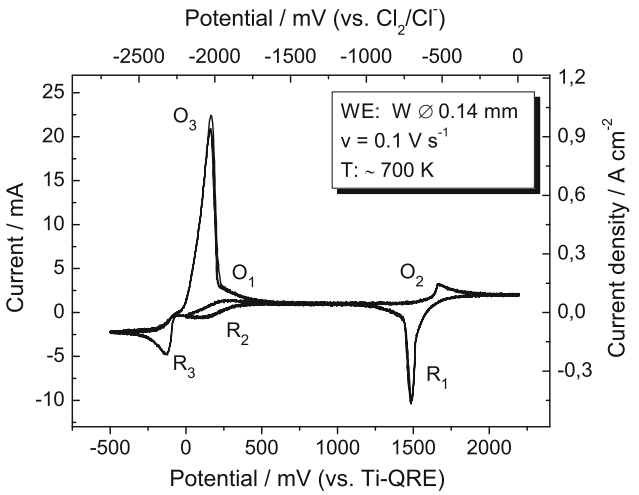

Fig. 2 CV in LiCl–KCl with 1 mol% $TiCl_2$ using tungsten to observe electrochemical reactions without interactions with the substrate: deposition (R_3) and dissolution (O_3) of titanium, reactions of divalent and trivalent titanium (O_1, R_2) and formation (O_2) and dissolution (R_1) of an unsolved compound

Additional peaks appeared when SCS-6 was used as the working electrode, but they were difficult to identify because of strong ohmic distortions (Fig. 3). We observed an almost linear slope (R_5) for the deposition process, and no peak or limiting current could be reached. A nucleation crossover (E_{CO}) indicated that some titanium had been deposited. The suspected lithium intercalation process could not be distinguished from titanium deposition and reduction of trivalent titanium by CV. In addition, the lithium intercalation process could not be differentiated from reduction of trivalent titanium ions and TiC

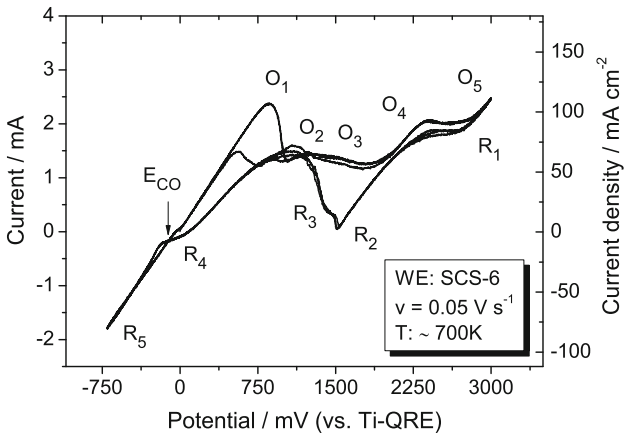

Fig. 3 CV in LiCl–KCl with 1 mol% $TiCl_2$. The CV is distorted due to the high ohmic resistivity of SCS-6

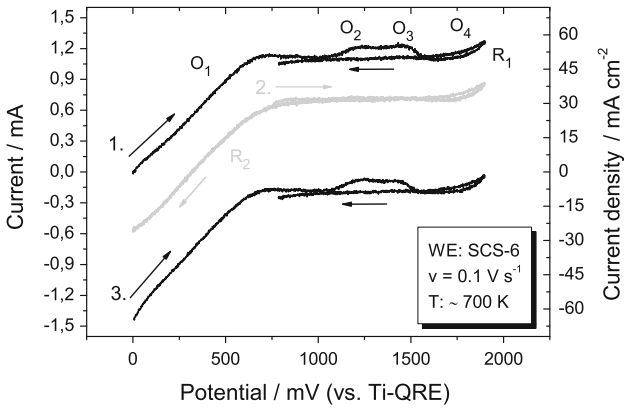

Fig. 4 CV in LiCl–KCl with 1 mol% $TiCl_2$ using SCS-6 as working electrode to demonstrate TiC decomposition. The curve without O_2 and O_3 corresponds to the second scan where the reverse potential (E_{Rev}) was 750 mV. The second and third curves are displaced in the diagram to allow a better discrimination of the scans. The CV is distorted due to the high ohmic resistivity of SCS-6. Oxidation of trivalent titanium (O_4) was only investigated up to low current densities to avoid the formation of unsolved products

formation. The assumption that TiC was formed and dissociated (according to Eq. 2) at SCS-6 and GC was supported by the oxidation peaks O_2 and O_3. These features could only be observed if carbonaceous substrates were used.

$$TiC \leftrightarrow Ti^{3+} + C + 3e^- \quad (2)$$

By investigating a smaller voltage range, peaks O_2 and O_3 became more distinct. Figure 4 shows that both of these peaks only appeared if the cathodic reverse potential (E_{Rev}) was sufficiently negative. The results acquired in LiCl–KCl–$TiCl_2$ using carbonaceous electrode materials were not completely in agreement with the findings of Popov et al. [15]. Popov et al. observed a reduction peak and assumed that it was associated with TiC formation at a more positive potential than that associated with the

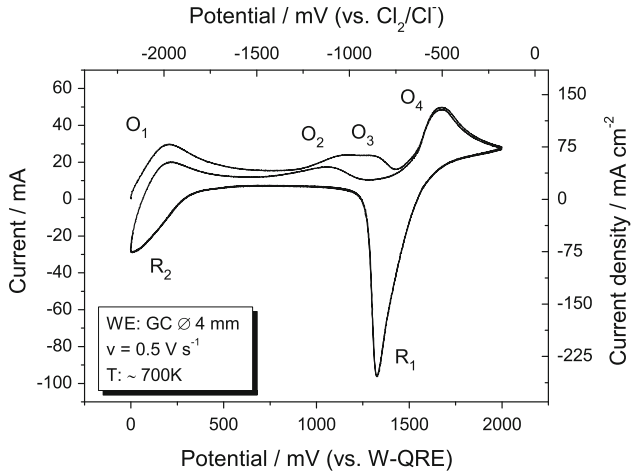

Fig. 5 CV in LiCl–KCl with 1 mol% $TiCl_2$ using GC as working electrode to demonstrate TiC decomposition. O_3 only appeared in the first scan, and O_2 was much smaller in the second and third scans, which indicated that TiC could also be chemically formed before the start of the electrochemical experiment

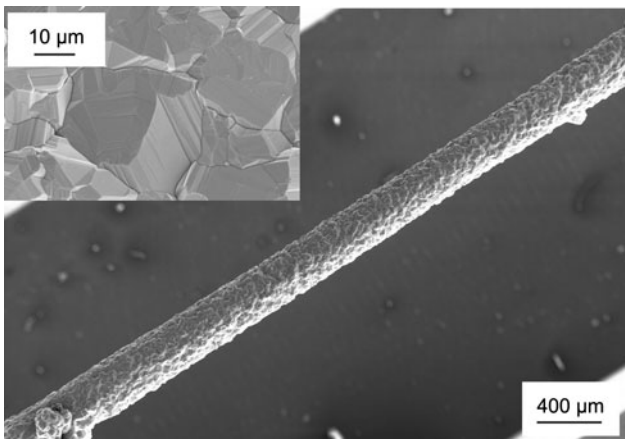

Fig. 6 SEM picture of titanium deposited on SCS-6 in LiCl–KCl with 1 mol% $TiCl_2$ at 700 K. Pulse parameters: $I_p = 2$ mA, $i_p \approx 80$ mA cm^{-2}, $t_{on} = 2.5$ ms, $t_{off} = 7.5$ ms. The current efficiency was approximately 85%. *Inset*: High magnification of the titanium coating with well-coalesced crystals

reduction of Ti(III). Furthermore, Popov et al. observed only one oxidation peak, similar to peak O_2 of the second CV scan in Fig. 5, which was performed with GC. The second peak (O_3) only occurred during the first scan after the electrode had remained non-polarised for longer periods of time. Additionally, peak O_2 was much smaller in the second scan. This demonstrates that TiC can also be formed at carbon electrodes that are simply dipped in the electrolyte. In the case of SCS-6, we observed two peaks that were independent of the order of the scan. The peaks were very similar in the first and third scans (Fig. 4, upper and lower curves, respectively).

Some measurements were also performed in LiCl–KCl with 2 mol% K_2TiF_6. According to Chen et al. [17] the LiCl–KCl–K_2TiF_6 electrolyte should not contain significant amounts of divalent titanium. When SCS-6 was used as working electrode, a peak has been observed that was probably corresponding to TiC formation. The peak could be observed in the fluoride containing electrolyte because there was no superposition with the reduction of trivalent titanium to divalent titanium.

3.2 Electrodeposition

The aim of the electrodeposition experiments was to find suitable parameters for the development of a fibre coating process. Applicable parameters were temperatures between 700 and 800 K, concentrations between 0.5 and 1 mol% $TiCl_2$ and average current densities between 10 and 50 mA cm^{-2}. The voltage was recorded to interpret events during electrodeposition. However, the voltage change (mainly a decrease) during the deposition process could not be definitively interpreted. The ohmic resistance of the SiC fibre was the main contribution to the measured voltage drop, especially at higher currents. This was established by experiments with tungsten wires that were conducted for comparison. Time-dependent contributions were nucleation, change of conductivity of the immersed portion of the fibre due to the growing titanium coating and decrease of current density due to enlargement of the surface because of the growing fibre diameter as well as morphological effects. "Short circuits" caused by foils and titanium networks on the surface of the molten salt (see Sect. 3.3.1) could only be recognised phenomenologically in some cases because generally, it was not a sudden process but a progressive process, and there was a more or less continuous voltage decrease.

3.3 Characterisation of the deposits

3.3.1 Morphology

In morphological studies, we found uniform coatings with constant thicknesses. The coatings were as thick as 80 µm, and there was no indication that it is not possible to realise even much thicker coatings (Fig. 6).[5] Despite large grains, the well-crystallised, dense coatings were rather smooth. However, compared to PVD coatings with similar coating thicknesses (both coatings were approximately 20-µm thick), the surfaces of the electrodeposited titanium coatings appeared quite rough. Although a simple arrangement

[5] The example depicted in Fig. 6 was created using pulse plating (peak current: I_p, peak current density: i_p, time in which there is a current: t_{on} and time without current: t_{off}). However, under the conditions studied, the pulses did not significantly change the morphology.

of two cylindrical electrodes placed in a distance of approximately 20 mm was used, the concentricity deviation was minor in cross-sections, which indicates that the throwing power of the electrolyte was good.

The deposits often exhibited growth failures like excrescences and foils or networks at the upper surface of the electrolyte. The excrescences had a polycrystalline structure, which was remarkable because re-nucleation does not seem to occur during the deposition process. An astonishing explanation for this observation was that there existed very thin oxygen-rich titanium foils (nanometre scale) that merged with the fibre during the deposition process. As a consequence of the electrical contact with the negatively polarised SiC fibre, nucleation and growth of titanium occurred on these foils, and finally, the foils were completely covered with titanium.

The morphologies of the coatings did not indicate tendencies of isolated crystal growth or dendrite formation. This observation was important because several papers have denied the suitability of all-chloride melts for the deposition of coherent titanium coatings (e.g. [18–20]). However, promising results from all-chloride melts have also been published by Haarberg et al. and Duan et al. [6, 21]. Excrescences can result in very complex entities, and the finding that these formations were completely coated with titanium indicates that the covering power of the electrolyte was good under the chosen conditions. The challenge is to avoid particles or foils that float in or on the electrolyte and that touch the fibres. One may consider using a cylindrical tungsten mesh around the electrode that prevents contact with such foils or particles in the electrolyte. Oxygen-rich titanium foils may be avoided by improving the purity of the electrolyte before adding $TiCl_2$. Apart from the formation of oxygen-rich foils, the impact of the impurity content of the electrolyte on the morphology and purity of the coating requires further studies. There is no consistent information in literature, but we favour the assumption that a high-purity electrolyte positively affects the morphology of titanium deposits [22].

Foil formation also occurred in experimental series without significant amounts of excrescences. Such foils have already been reported in the literature and may not be avoidable in all-chloride melts. Kühnl et al. [23] proposed cathode shielding to stop the growing foils. In this study, we observed various forms of foils and titanium networks (e.g. Fig. 7). Although there is no general explanation for all observed phenomena, we know that they cannot be explained by the high ohmic resistance of SCS-6 because foils also formed at tungsten.

In some SEM studies, microscopic growth failures could also be observed (Fig. 8). Hexagonal structures formed on basal planes, and some planes had cleavages, which resulted in a schist-like appearance. Currently, no explanation or solution is available for this type of failure, and the consequences on mechanical properties have not been investigated.

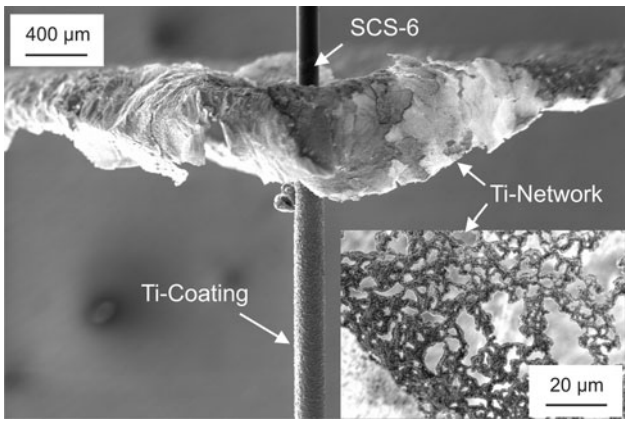

Fig. 7 SEM picture of a titanium network grown on the surface of the electrolyte during electrodeposition of titanium on SCS-6 in LiCl–KCl with 0.5 mol% $TiCl_2$ at 700 K. The current density was approximately 25 mA cm^{-2}. *Inset*: High magnification of titanium network

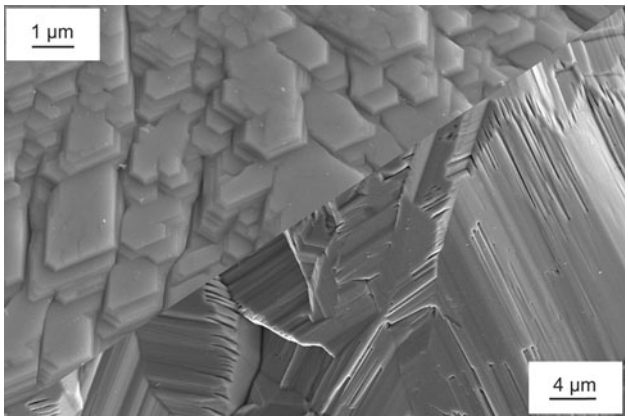

Fig. 8 SEM pictures of microscopic growth failures observed in titanium deposits grown on SCS-6 in LiCl–KCl with 1 mol% $TiCl_2$ at 700 K. Pulse parameters: $I_p = 2$ mA, $i_p \approx 120$ mA cm^{-2}, $t_{on} = 2.5$ ms, $t_{off} = 7.5$ ms. Hexagonal structures (*top left*) and cleavages (*bottom right*)

3.3.2 *Microstructure*

The microstructure was investigated using optical microscopy and SEM. In addition, EBSD was applied to characterise the MCFs. Generally, columnar grains could be observed in cross-sections, and some cases exhibited thin, elongated plains (probably growth twins). We also observed a coarsening of grains from the substrate to the surface due to faster grains growing at the expense of slower grains. This result could be confirmed by nucleation studies, which demonstrated a high density of nuclei. Despite smoother surfaces, PVD coatings of pure titanium,

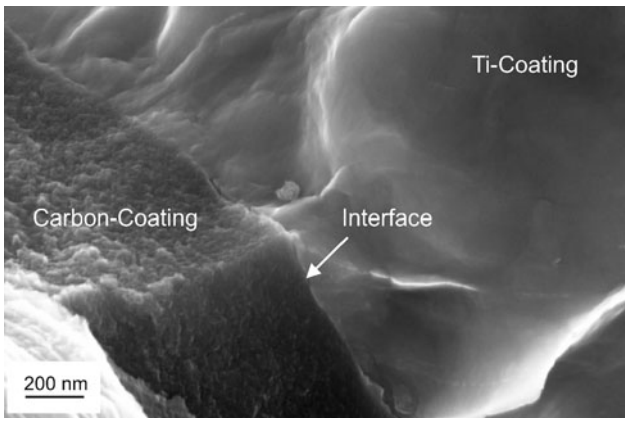

Fig. 9 SEM picture of the interface between the outer carbon coating of SCS-6 and a titanium coating grown in LiCl–KCl with 1 mol% $TiCl_2$ at 700 K. Pulse parameters: $I_p = 2$ mA, $i_p \approx 80$ mA cm^{-2}, $t_{on} = 2.5$ ms, $t_{off} = 7.5$ ms. The coated fibre was broken by bending

which were analysed for comparison, had similar grain sizes but did not exhibit sharp crystal faces.

3.3.3 Fractography

A fibre with an 80-μm thick titanium coating was broken by bending the coated portion. The fracture behaviour appeared ductile. At very high magnifications (SEM), the interface could be analysed (Fig. 9), and we observed complete coverage and good adhesion of titanium on the outer carbon coating of SCS-6. No evidence of negative influences of lithium intercalation or TiC formation could be found. In fact, a small amount of TiC formation should have a reinforcing effect on the adhesion of titanium to SCS-6.

4 Conclusions and outlook

In this study we investigated electrodeposition of titanium, namely the specifics resulting from the properties of SCS-6 used as substrate. Although the cyclic voltammagrams were distorted because of high ohmic resistance of SCS-6, they could be interpreted by choosing GC and tungsten as references. Titanium carbide formation occured at a potential close to that associated with the reduction of trivalent titanium. When using SCS-6 as working electrode, lithium intercalation started at potentials that were even more positive than in the experiments with GC. Therefore, intercalation can be expected to take place during nucleation and growth of nuclei as long as no compact titanium layer covers the carbon surface. The effects of lithium intercalation are not yet known, but there may be consequences on mechanical properties. Microscopic growth failures, which have been observed in the SEM studies, may be even more important. Indeed, these growth failures may be critical if some electrolyte is incorporated during the electrodeposition process.

Critical effects of fibre characteristics on the morphology could not be substantiated. Dense and uniform coatings with good adhesion were fabricated, whereas the formation of foils, excrescences and microscopic failures were independent of the substrate. In addition, we demonstrated that there was no needle or dendrite growth mechanism. Therefore, the utilisation of an all-chloride electrolyte seems appropriate. However, due to the high ohmic resistivity, the coating of longer fibres may require special measures, such as a translational movement of the substrate. A future goal will be to develop of a continuous fibre coating process.

Acknowledgment The support of the project by the Helmholtz Association of German Research Centers within the Helmholtz-University Young Investigators Group "Electrolytical Production Routes for Titanium Matrix Composites" is acknowledged.

References

1. Leyens C, Hausmann J, Kumpfert J (2003) Adv Eng Mater 5:399
2. Vassel A (1999) Mater Sci Eng A 263:305
3. Lantelme F, Salmi A, Coffin B et al (1996) Mater Sci Eng B 39:202
4. Lantelme F, Kuroda K, Barhoun A (1998) Electrochim Acta 44:421
5. Lantelme F, Salmi A (1995) J Electrochem Soc 142:3451
6. Haarberg GM, Rolland W, Sterten Å et al (1993) J Appl Electrochem 23:217
7. Martinez AM, Castrillejo Y, Barrado E et al (1998) J Electroanal Chem 449:67
8. Polyakova LP, Stangrit PT, Polyakov EG (1986) Electrochim Acta 31:159
9. Polyakova LP, Taxil P, Polyakov EG (2003) J Alloys Compd 359:244
10. Girginov A, Tzvetkoff TZ, Bojinov M (1995) J Appl Electrochem 25:993
11. Ward Y, Young RJ, Shatwell RA (2004) J Mater Sci 39:6781
12. Smith PR, Gambone ML, Williams DS et al (1998) J Mater Sci 33:5855
13. Dübgen R, Popp G (1984) Materialwiss Werkst 15:331
14. Ferry DM, Picard GS, Tremillon BL (1988) Trans Inst Min Metall C 97:21
15. Popov BN, Kimble MC, White RE (1991) J Appl Electrochem 21:351
16. Ferry DM, Picard GS (1990) J Appl Electrochem 20:125
17. Chen G-S, Okido M, Oki T (1988) J Appl Electrochem 18:80
18. Robin A, Ribeiro RB (2000) J Appl Electrochem 30:239
19. Ene N, Zuca S (1995) J Appl Electrochem 25:671
20. Mellors GW, Senderoff S (1965) J Electrochem Soc 112:266
21. Duan S, Gu X, Du Y et al (1989) Rare Metals 8:6
22. Ehrlich P (1957) Chem Ing Tech 29:557
23. Kühnl H, Ehrlich P, Uihlein RD (1960) Z Anorg Allg Chem 306:246